Integrating Competitive Bioassays and Mechanistic Models to Assess Environmental AMR Selection

Renu Bisht*, Matti Gralka, Yuval Mulla, Peter Cenijn, Timo Hamers, Rik Oldenkamp
Vrije Universiteit Amsterdam (NL)
*Correspondence: Renu Bisht (r.bisht@vu.nl)

Introduction

Antimicrobial resistance (AMR) is an escalating global health challenge driven not only by clinical antibiotic use but also by the environmental dissemination of antibiotic residues and resistance genes (ARGs) via wastewater and natural ecosystems[1]. Current approaches, such as the 8-day SELECT bioassay, infer AMR selection based on growth inhibition thresholds but do not explicitly capture competitive growth dynamics between susceptible and resistant bacteria, limiting mechanistic insight under environmentally relevant exposure conditions.

In this study, we focus on ciprofloxacin (CIP), a fluoroquinolone antibiotic that inhibits bacterial DNA gyrase and topoisomerase IV, thereby disrupting DNA replication and transcription. Due to its widespread use and incomplete metabolism, CIP is a prevalent aquatic contaminant that promotes the emergence and spread of AMR, posing risks to human health and ecosystems[2]. To address existing gaps in understanding resistance selection in microbial communities, we integrate experimental, genomic, and modeling approaches. First, we develop an *in vitro* coculture competition assay using fluorescently tagged wild-type and CIP-resistant *Escherichia coli (E.coli)* to directly quantify selection dynamics under ciprofloxacin exposure. The resulting coculture data are then combined with genomic information on resistance-associated mutations and their corresponding phenotypic mechanisms of resistance, to mechanistically capture kinetics and dynamics of fluoroquinolone action in an *in-silico* model. The resulting parameterized *in-silico* model would describe bacterial competition and antibiotic effects, enabling exploration of alternative exposure scenarios and would allow the extension of this model to other antibiotics and resistance mechanisms.

Together, this work will establish an experimentally grounded and mechanistically informed framework for assessing AMR selection in environmental contexts, enabling more robust prospective risk assessments for antibiotics and supporting improved environmental protection strategies.

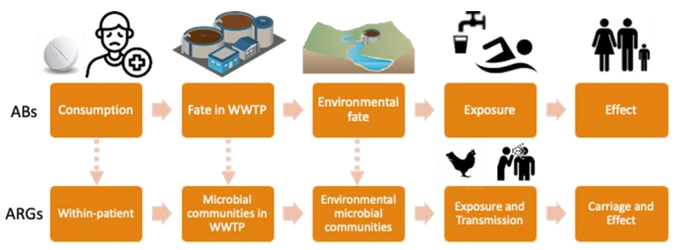

Fig. Showing parallel source-to-effect pathways of antibiotics (Abs) and antibiotic resistance genes (ARGs)

Objectives

- To develop a coculture bioassay to explicitly incorporate differential growth inhibition between wild-type (antibiotic-sensitive) and ciprofloxacin-resistant fluorescently tagged *E.coli* strains under antibiotic exposure. This approach will establish an experimental endpoint that more accurately reflects AMR selection, rather than simple inhibition or survival
- To integrate data from mono- and coculture bioassays with genomic information on resistance-associated mutations, in order to parameterize a mechanistic *in silico* model of bacterial growth and competition under antibiotic exposure. This framework will enable exploration of alternative exposure scenarios and extension to additional antibiotics and resistance mechanisms

Methodology

1. Construction of ciprofloxacin-resistant fluorescently tagged *E.coli* strains with Adaptive laboratory evolution (ALE)

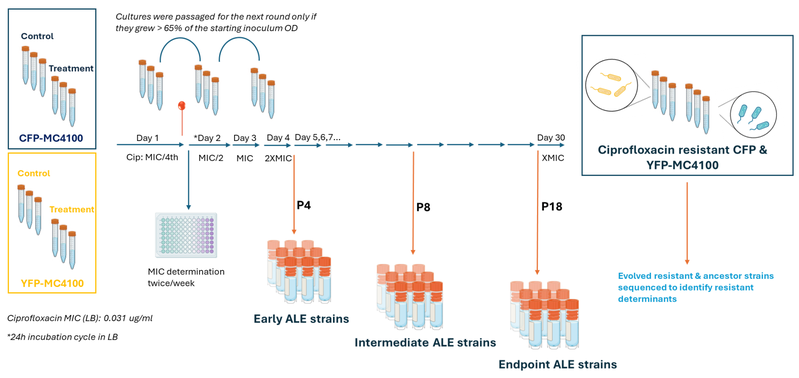

Fig. 1. Adaptive laboratory evolution (ALE) of ciprofloxacin-resistant CFP- and YFP-tagged *E.coli* MC4100
CFP- and YFP-tagged E. coli populations (three replicates) were evolved in parallel under control conditions or ciprofloxacin treatment using serial passaging with increasing drug concentrations. Samples were collected at three evolutionary stages (P4, P8, and P18; passage numbers), representing early, intermediate, and endpoint lineages that harbor progressively increasing levels of resistance, ranging from low-level, nonspecific tolerance (P4) to high-level, ciprofloxacin-specific resistance (P18)

2. Strain(s) characterization and minimum inhibitory concentration (MIC) determination

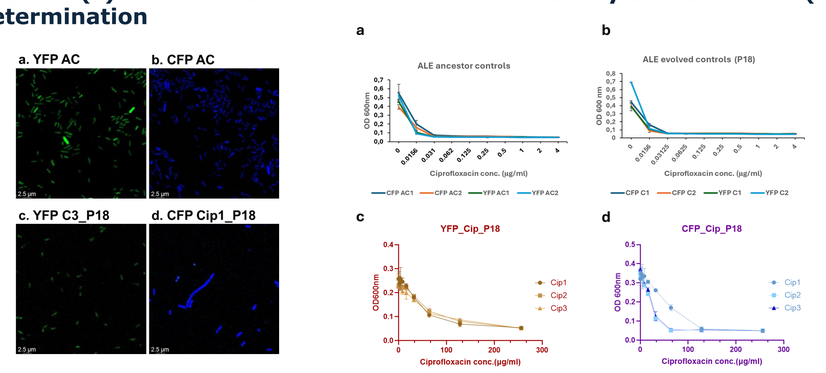

Fig. 2. Ciprofloxacin-evolved and ancestor ALE strain(s) characterization
(Left) Confocal microscopy images showing expression and cellular morphology of CFP- and YFP-tagged E. coli strains, including ancestral controls (AC), evolved controls (C3), and ciprofloxacin-treated ALE strains (Cip1) at p18. (Right) Ciprofloxacin susceptibility (MIC determination) of ancestral controls (AC), ALE-evolved controls (C), and ciprofloxacin-evolved strains (Cip). Panels (a–b) show dose–response curves for AC and evolved control strains, while panels (c–d) show control YFP-tagged and ciprofloxacin-treated CFP-tagged P18 strains

Results

3. Susceptibility of ALE-ciprofloxacin evolved *E.coli* strains against different classes of fluoroquinolones

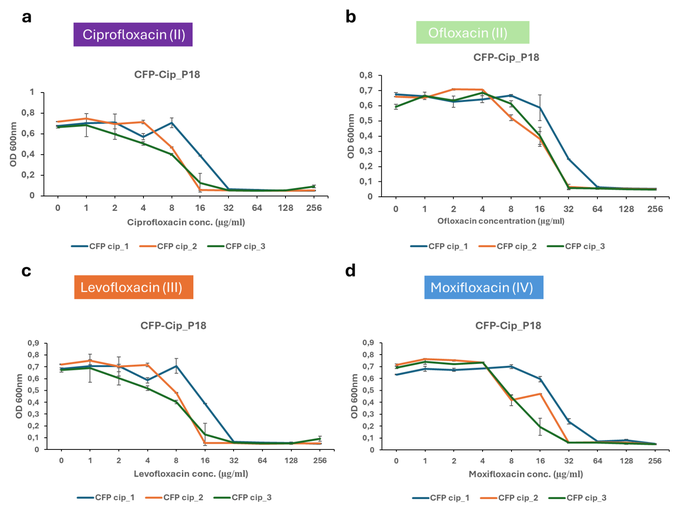

Fig. 3. Dose response growth profiles of ciprofloxacin-evolved CFP-tagged *E.coli (P18)* exposed to fluoroquinolones
Dose–response growth profiles of ciprofloxacin-evolved E. coli (CFP-tagged, passage 18) exposed to fluoroquinolones from different generations (II-IV) (ciprofloxacin, ofloxacin, levofloxacin, moxifloxacin), showing patterns of cross-resistance. The MIC of ALE ancestor control for CFP-tagged E.coli was 0.0031 ug/ml (Ciprofloxacin), 0.125 ug/ml (Moxifloxacin), 0.0625 ug/ml (Levofloxacin) and 0.125 ug/ml (Ofloxacin) (data not shown)

4. Growth dynamics of resistant-CFP and susceptible-YFP-tagged ALE *E.coli* strains

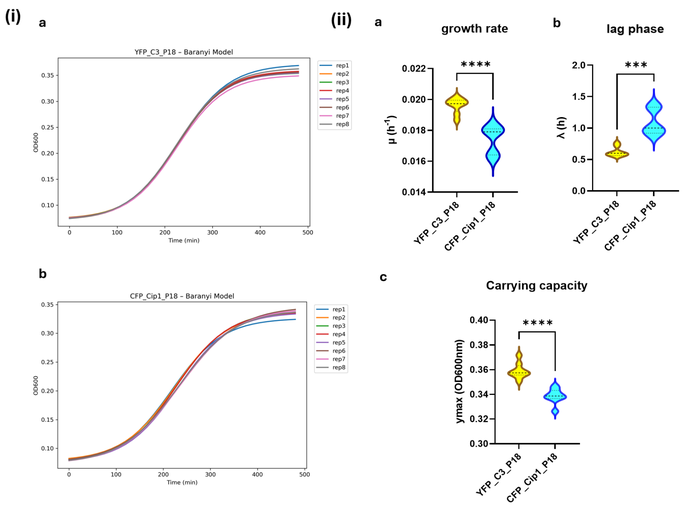

Fig. 4. Growth dynamics of CFP and YFP-tagged ALE evolved strains
Growth dynamics of control YFP-tagged (a) and ciprofloxacin-evolved CFP-tagged E.coli P18 strains (b) were modeled using the Baranyi growth model (in LB media) (ii) Violin plots show the distribution of estimated growth parameters derived from Baranyi model fits for CFP-ciprofloxacin resistant (blue) and YFP-sensitive (yellow) ALE-evolved strains. Statistical comparisons between CFP (resistant) and YFP (sensitive)-tagged E.coli strains were performed using an unpaired parametric two-sample t-test with Welch's correction for unequal variances.

5. Whole genome sequencing (WGS)-based identification of resistant determinants in ALE-evolved ciprofloxacin resistant *E.coli* strains using BRESEQ

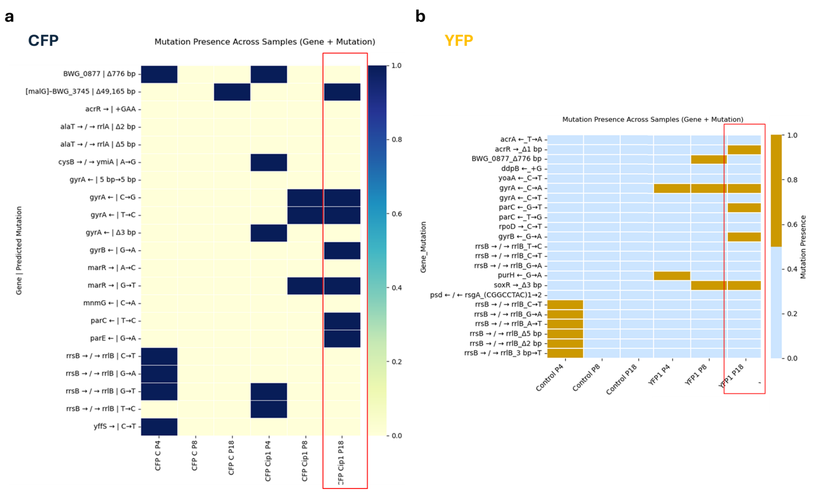

Fig. 5. Breseq-based mutation profiles of evolved CFP and YFP strains
Heatmaps depict mutations identified using Breseq tool across control and ciprofloxacin-treated populations at passages P4, P8, and P18 for CFP (a) and YFP (b) tagged E.coli lineages. Rows represent individual mutations (gene and mutation type), and columns represent strains. Color intensity indicates mutation presence (0 = absent, 1 = present). Red boxes highlight P18 lineage (the endpoint ALE evolved strains).

6. Competition coculture bioassay and minimum selective concentration (MSC) determination

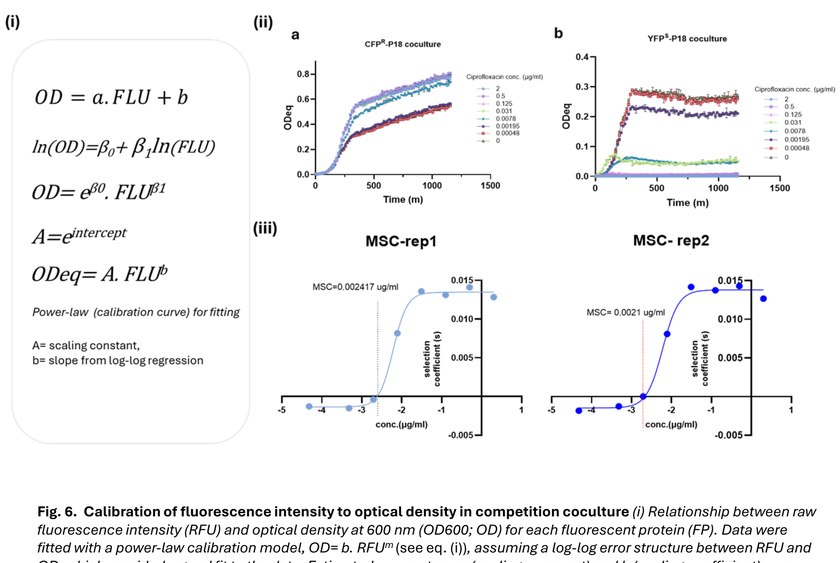

Fig. 6. Calibration of fluorescence intensity to optical density in competition coculture *(i) Relationship between raw fluorescence intensity (RFU) and optical density at 600 nm (OD600; OD) for each fluorescent protein (FP). Data were fitted with a power-law calibration model, OD= b. RFU^m* (see eq. (i)), *assuming a log-log error structure between RFU and OD, which provided a good fit to the data. Estimated parameters m (scaling exponent) and b (scaling coefficient) were used to convert RFU to optical density equivalents (ODeq). Competition experiment was performed at varied concentration of ciprofloxacin with a 1:1 ratio of CFP^R vs YFP^S P18 strains in LB media in 96 well plate for 20 h with two technical replicates (rep1 & rep2). MSC was calculated as the concentration at which the fitted selection coefficient (derived from the log ratio of CFP/YFP in coculture) crosses zero (s=0). The MSC for rep 1 was estimated at* ***2.4 µg/L (95% CI: 1.4–4.2 µg/L).***

Summary

❑ *E.coli* MC4100 strains, tagged chromosomally with *cfp* and *yfp* markers were evolved in the laboratory under gradually ciprofloxacin concentrations, resulting in three independent lineages (P4, P8, and P18) with varying degrees of resistance, ranging from low- to high-level ciprofloxacin-specific resistance (**fig. 1 & 2**). The MICs of the ALE endpoint strains (P18) were in the range of 16–64 µg/mL, representing approximately 500–2000-fold increase compared to the sensitive ancestral (or evolved control) strain.

❑Ciprofloxacin-evolved CFP-tagged *E. coli* (P18) exhibited broad cross-resistance to fluoroquinolones (II–IV generations), with right-shifted dose–response curves and sustained growth at higher antibiotic concentrations compared to the susceptible ancestor (or evolved control) (data not shown) (**fig. 3**). MIC values ranged from 16–32 µg/mL across all tested antibiotics, indicating a consistent, broad fluoroquinolone resistance phenotype comparable to ciprofloxacin. The uniform shift in susceptibility profiles suggests cross-resistance mediated by shared targets, including DNA gyrase and topoisomerase IV. Variation among replicates indicate heterogeneity in resistance levels within evolved populations.

❑ALE endpoint strains (CFP-Cip1_P18) exhibited reduced growth rate, longer lag-phase, and lower carrying capacity as compared to their corresponding control strains (YFP-C3_P18), with similar trends observed in the P8 lineage (data not shown), indicating a fitness cost associated with the acquisition of ciprofloxacin resistance (**fig. 4**).

❑Evolved strains (P18) acquired mutations in key fluoroquinolone resistance genes (*gyrA*, *parC*, *gyrB*) and regulatory elements (*marR*, *acrR*), along with additional mutations in stress-response and membrane-associated pathways (**fig. 5**). Target-site mutations were consistently enriched in endpoint populations, supporting a mechanistic basis for resistance and cross-resistance. Distinct mutation profiles between CFP and YFP lineages, and across replicates, indicate parallel evolution with lineage-specific adaptations and genetic heterogeneity.

❑The MSC for ciprofloxacin was estimated at 0.0024 µg/mL, which is ~13-fold lower than the MIC (0.031 µg/mL) of the susceptible strain in LB media. This demonstrates that selection for resistant populations occurs well below inhibitory concentrations, highlighting that even very low, sub-MIC levels of ciprofloxacin can drive resistance enrichment (**fig. 6**).

Future prospectives

- ❑ Integrate mono- and coculture data across passages (P4, P8, & P18) with whole-genome sequencing to link resistance-associated mutations to phenotypic AMR mechanisms
- ❑ Develop a mechanistic *in-silico E. coli* model capturing ciprofloxacin and fluoroquinolone kinetics and dynamics, including intracellular accumulation, target binding, and growth inhibition
- ❑ Explicitly incorporate distinct resistance mechanisms, such as target site alterations in higher-MIC strains (P18) and more generic efflux-based mechanisms in lower-MIC strains (P4)
- ❑ Extend the modeling framework to additional antibiotics and classes, creating a virtual multi-drug resistant *E.coli* model that can be used to predict MSCs enabling predictive assessment of selection thresholds to support environmental AMR risk assessment

References

1. La Rosa, M. C., Maugeri, A., Favara, G., La Mastra, C., Magnano San Lio, R., Barchitta, M., & Agodi, A. (2025). The Impact of Wastewater on Antimicrobial Resistance: A Scoping Review of Transmission Pathways and Contributing Factors. *Antibiotics*, *14*(2), 131. https://doi.org/10.3390/antibiotics14020131
2. Al-howri, B.M., Ismail, S. & Khajavian, M. comprehensive review of ciprofloxacin pollution in water: sources, environmental impacts, remediation techniques, and research challenges. *Environ Monit Assess* **197**, 1095 (2025). https://doi.org/10.1007/s10661-025-14454-z
3. Barrick, Jeffrey E et al. "Identifying structural variation in haploid microbial genomes from short-read resequencing data using breseq." BMC genomics vol. 15,1 1039. 29 Nov. 2014, doi:10.1186/1471-2164-15-1039
4. Kehila D, Tokuriki N.2024.Measuring differential fitness costs and interactions between genetic cassettes using fluorescent spectrophotometry. Appl Environ Microbiol90:e01419-23.https://doi.org/10.1128/aem.01419-23